J. Biomed. Eng. Res.
Vol.26, No.1, 43-47, 2005

Development of a Small Animal CT using a Linear Detector Array and Small-Scale Slip Rings

Ung Hwan An, In Kon Chun, Sang Chul Lee, Min Hyoung Cho, Soo Yeol Lee

Dept. of Biomedical Engineering, Kyung Hee University, Korea
(Received September 23, 2004. Accepted December 9, 2004)

Abstracts: We have developed a small bore x-ray CT for small animal imaging with a linear x-ray detector array and small-scale slip rings. The linear x-ray detector array consists of 1024 elements of 400 μm×400 μm with a gadolinium oxysulfide (GOS) scintillator on top of them. To avoid use of expensive large diameter slip rings for projection data transmission from the x-ray detector to the image reconstruction system, we used the wireless LAN technology. The projection data are temporally stored in the data acquisition system residing on the rotating gantry during the scan and they are transmitted to the image reconstruction system after the scan. With the wireless LAN technology, we only needed to use small-scale slip rings to deliver the AC electric power to the X-ray generator and the power supply on the rotating gantry. The performances of the small animal CT system, such as SNR, contrast, and spatial resolution, have been evaluated through experiments using various phantoms. It has been experimentally found that the SNR is almost linearly proportional to the tube current and tube voltage, and the minimum resolvable contrast is less than 30 CT numbers at 40kVp/3.0mA. The spatial resolution of the small animal CT system has been found to be about 0.9 lp/mm. Postmortem images of a piglet is also presented.

Key words: X-ray CT, Performance evaluation, Small animal imaging, Linear detector array, Contrast, Spatial resolution

INTRODUCTION

Necessity of small animal imaging modalities has been growing fast to support recent developments in bio-technology [1]. When we use human imaging modalities in small animal imaging, it is inevitable to suffer from poor spatial resolution and low SNR due to smaller physical size of the animal. To optimize the imaging performance in small animal studies, many kinds of small animal imaging modalities, such as mini-PET, mini-SPECT and mini-MRI, have been developed [2-4]. It is expected that the small animal imaging modalities will play great roles in developing new medicines and in investigating new treatment technologies with small animal models.

X-ray computed tomography (CT) has been widely used for clinical imaging owing to its superb spatial resolution and fast scan capability. However, small animal x-ray CT systems have not been developed mainly due to the high cost of x-ray detectors and rotating gantry mechanisms employed in clinical x-ray CT systems. If small animal x-ray CT systems are affordable, it is expected that the small animal x-ray CT can be greatly used for combinatory studies with other imaging modalities.

In this study, we introduce a small bore helical x-ray CT with the field of view (FOV) of 20cm. For fan-beam mode projection data acquisition, we used a linear x-ray detector array with sequential read-out capability, and a low power x- ray tube with a static target. We present small animal imaging results together with performance analysis results such as SNR, contrast, and spatial resolution evaluated with various kinds of phantoms.

This work supported by a grant of KISTEP, Republic of Korea (M2-0305-04-0005)
Corresponding Author: Soo Yeol Lee, Professor
Dept. of Biomedical Engineering, Kyung Hee University
1 Seochon, Kiheung, Yongin, Kyungki 449-701, Korea
Tel. +82-31-201-2980 Fax. +82-31-201-3666
E-mail. sylee01@khu.ac.kr

MATERIALS AND METHODS

Small Animal X-ray CT System

A schematic diagram of the developed small-animal x-ray CT is shown in figure 1 and a photograph of the system in figure 2. The system consists of an x-ray source and a linear x-ray detector array mounted on a rotating gantry, a gantry control unit and a parallel

image reconstruction unit. The x-ray source (SM-20HF, Listem, Korea) is a sealed tube with a fixed tungsten anode having an angle of 12° against the electron beam and a 0.6mm focal spot size. The maximum tube voltage and tube current are 110kVp and 3.0mA, respectively. Using the low-power static-target x-ray tube rather than a conventional x-ray CT tube with a rotating anode, we can reduce the system size significantly. However, we have longer scan time due to the low power capacity of the x-ray tube. The linear x-ray detector array (X-scan 0.4f, Detection Technology, Finland) is designed for non-destructive testing in the range of 30~160 kVp. The x-ray detector has a built-in sequential read-out circuit with a 14 bit A/D converter. The number of detector elements is 1024 and the element size is 400□m×400□m. The incoming x-rays are first converted to visible light by the scintillator layer and the visible light is converted to the electrical signal by the photo diode array. The scintillator layer is made of gadolinium oxysulfide (GOS) with the thickness of 400□m. Each sensitive element of the detector provides an electrical signal proportional to the flux and energy of the x-rays absorbed in the element.

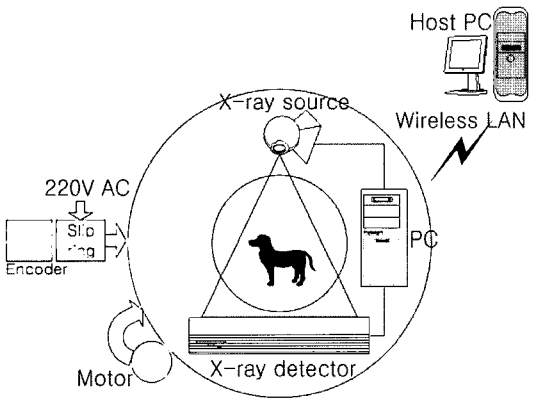

Fig. 1. A schematic diagram of the x-ray CT system

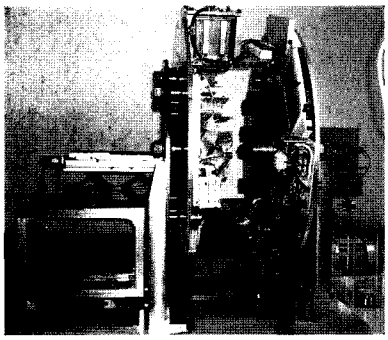

Fig. 2. A photograph of the x-ray CT system

The x-ray source and the detector are mounted on a circular gantry made of 18mm thick aluminum plate. The ring diameter and source-to-detector distance are 1300mm and 1000mm, respectively. The couch with the size of 600mm×150mm was made of carbon film. The couch movement is actuated by a servo motor under the control of the host PC which handles the helical scan parameters such as helical pitch and rotating speed of the gantry.

The gantry is rotated by a 1.5kW, 3 phase 220V AC motor with the belt and pulley mechanism. The rotating speed of the gantry can be controlled from 3 to 30 RPM. A data acquisition system (DAS) is also mounted on the gantry. The DAS acquires the projection data from the linear detector and stores them temporarily during the scan. The acquired scan data are then transferred to the image reconstruction unit through the wireless LAN. The electrical power for the x-ray tube, the x-ray detector and the DAS is delivered through slip rings. Since we use wireless data transmission technique to transfer the projection data to the image reconstruction unit, we are able to use small-scale slip rings in which the number of contacts is only 5. For the data acquisition and x-ray source and detector control, we used a PC (Pentium IV 2.4GHz). The PC also handles the data transmission to the image reconstruction unit through the wireless LAN.

We used the fan-beam mode filtered back-projection algorithm to reconstruct images from the projection data. For fast image reconstruction, we used the look-up table method in calculating the fan-beam mode weighting factor and the ray indices [5]. The projection data were acquired in the matrix form of 1024×Nv, where is Nv is the number of views.

Projection data with 300~1200 views has been usually acquired, and it takes about 16 seconds to reconstruct a 512×512 image from 1200 projection data (with Pentium4 2.4GHz). For the image reconstructions, the Ram-Lak filter has been used for filtering the projection data before back-projections [6]. The images were reconstructed in the matrix form of 512×512 or 1024×1024 depending on applications. When we reconstruct the image in the 1024×1024 matrix form, the pixel size is 200□m. The maximum FOV of the system is 200mm with the maximum helical scan length of 400mm.

Performance Evaluation

All the performance evaluations of the x-ray CT have been performed with the image magnification ratio of 2:1, the gantry rotating speed of 20 RPM, the detector integration time of 2.5msec and the Al filter thickness of 0.5mm. To compensate the detector non-uniformity and bad pixel effects, we obtained a white reference projection data and a dark current reference data. For the reference data, we took the average of 1200 scans. After obtaining the reference data, each

projection data was subtracted by the dark current reference data and then divided by the white reference projection data.

To evaluate the SNR characteristic, we used a cylindrical phantom filled with water as shown in figure 3(a). After reconstructing 2D images, SNR was calculated by dividing the mean intensity value by the standard deviation of the intensity values in the given area.

We tested low-contrast visibility using a contrast phantom shown in figure 3(b). The contrast phantom consists of six inserts whose physical densities are similar to that of water. The six inserts with 5mm diameter were immersed in a water bath made of a 40mm diameter acrylic cylinder. The inserts were made of commercial electron density phantoms (Model 76-430, Nuclear Associates, USA). Physical properties of the six inserts are shown in table 1. The contrast phantom was imaged in various dose levels, and the minimum dose level to differentiate the low-contrast inserts was determined.

We have evaluated the spatial resolving power of the small-animal CT system using a 60 m thick wire placed in the middle of an acrylic cylinder. The wire images were acquired with the pixel size of 200×200 m2. Assuming the wire image is the point spread function, we calculated the MTF of the x-ray CT by taking the Fourier transformation on the point spread function [7]. The calculated MTF represents the total system MTF which reflects various physical parameters such as the focal spot size, the magnification ratio, the reconstruction algorithm and the detector resolving power [8].

Soft tissue and bony structure visibility tests were performed by imaging a piglet postmortem. Abdomen image was obtained at 60kVp and 3.0mA in the helical scan mode. The slice thickness was 0.4mm and the helical pitch was 1.0 mm. For the helical mode image reconstruction, we used the full scan mode image reconstruction algorithm [9].

Table 1. Physical properties of the inserts in the contrast phantom

index	Material	Physical density (g/cm3)	Mean CT# at 60kVp
A	Plastic water	1.030	383.2
B	Nylon	1.150	-47.7
C	Polyethylene	0.950	-203.8
D	Acrylic	1.180	-2.6
E	Polystyrene	1.110	-166.6
F	Polycarbonate	1.180	-35.5

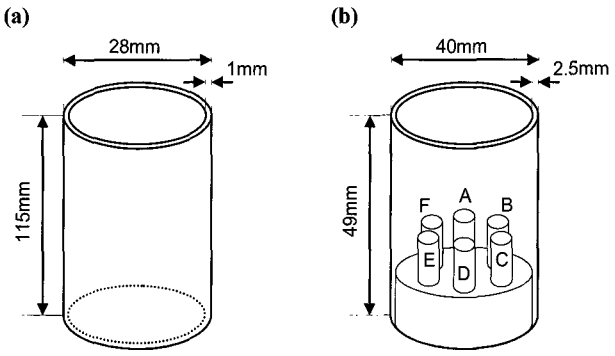

Fig. 3. Phantoms used in the performance evaluation. (a) The uniform water phantom for SNR evaluation. (b) The contrast phantom for CNR evaluation.

EXPERIMENTAL RESULTS

Figure 4 shows SNRs measured from the uniform water phantom images taken with various combinations of kVp and mA. The SNR is almost linearly proportional to the tube current, and the higher tube voltage gives the better SNR owing to high conversion efficiency of the high energy x-ray photon in the scintillator layer. If we set the low bound of SNR to 10, tube voltages higher than 60kVp at 3.0mA seems to be appropriate for soft tissue imaging.

Figure 5 shows a reconstructed image of the contrast phantom. As can be seen from the figure, all the inserts except the acryl insert are differentiated from the background water region. This demonstrates that the x-ray CT is capable of differentiating the contrast as small as 30 CT-numbers.

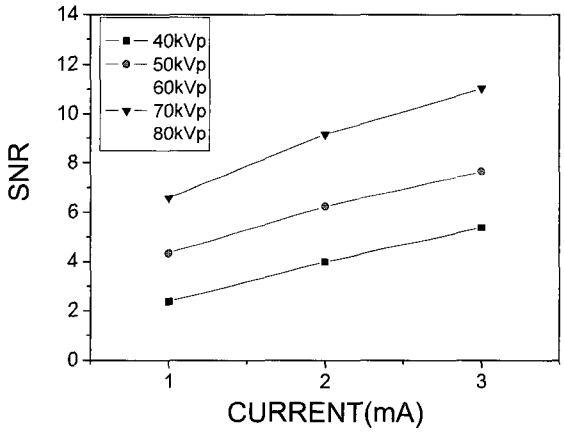

Fig. 4. SNRs with respect to the tube current and voltage.

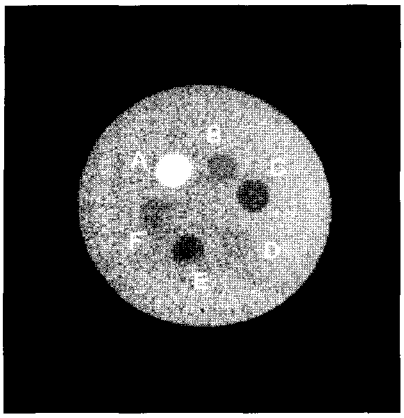

Fig. 5. A representative image of the contrast phantom obtained at 40kVp, 3.0mA and 20RPM

Figure 6(a) shows a reconstructed image of the wire phantom. We took a line profile at the middle of the wire and applied Fourier transform to the line profile to calculate the MTF. Figure 6(b) shows the calculated MTF of the x-ray CT.

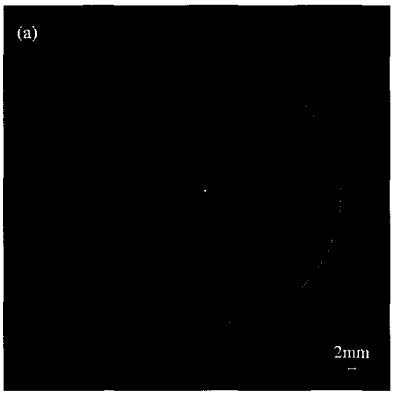

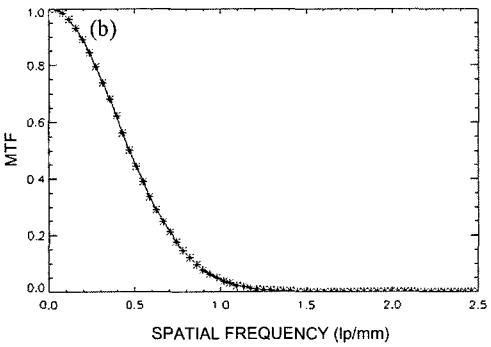

Fig. 6. (a) A representative image of the wire phantom. (b) The MTF of the x-ray CT system.

If we assume that the limiting spatial resolution corresponds to the point when the MTF drops to 10%, then we can infer that the spatial resolution limit of the x-ray CT system is about 0.9 lp/mm. Considering that the typical spatial resolution of medical CTs is 0.5 ~ 2.0 lp/mm [10], we think that the developed x-ray CT has enough resolution for small animal imaging

To test soft tissue visibility in small animal studies, we have obtained postmortem images of a piglet. One of representative images of the piglet is shown in figure 7 together with the scout viewing image. The cross-sectional image was obtained with the helical scan mode with the helical pitch of 2.5:1. The pixel size of figure 7(b) is 200×200μm2 with the matrix size of 1024×1024.

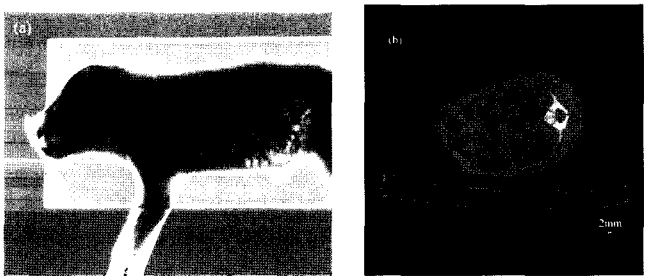

Fig. 7. (a) A scout viewing image of the piglet at 60kVp, 3.0mA, 10cm/sec. (b) A helical CT scan image of the piglet at 60kVp, 3.0mA, 10RPM, 1mm helical pitch.

DISCUSSIONS AND CONCLUSIONS

We have developed the x-ray CT system with minimal electronic circuitry by using a linear x-ray detector array. Owing to the serial readout capability of the linear detector array, we do not need to have many number of data acquisition electric circuitries which are commonly used in conventional medical CTs. By transmitting the projection data through wireless LAN, we were able to use small-scale slip rings with the number of rings being only 5. The experiment results have demonstrated that the developed x-ray CT can be used in small animal studies. However, we need to have further developments to optimize the x-ray CT system for small animal imaging especially in SNR performance. Due to the low power of the x-ray source, SNR of the developed system is much lower than conventional medical x-ray CTs. Even though the low SNR can be compromised with longer scan time, we still have to improve the SNR performance. Since we used the x-ray tube customized for x-ray radiography, the span angle of the fan-beam x-ray was only 12 degrees. If we use an x-ray tube having larger span angle, we can reduce the distance between the x-ray source and the detector, thus, reducing the gantry size and improving SNR performance. The pixel pitch of the detector was 400□m which made the slice thickness of 200□m at the magnification ratio of 2:1. The slice

thickness of 200 m seems to be rather too small for small animal studies. If we use a linear detector array with wider width in the slice direction, we can improve the SNR and CNR performances significantly.

In conclusion, we have developed an x-ray CT system for small animal imaging with minimal electronic circuitry. We expect that the developed x-ray CT system can be greatly used for in vivo small animal imaging studies in the near future.

REFERENCES

[1] Michael J. Paulus, Shaun S. Gleason, M. Evangeline Easterly, and Charmaine J. Foltz, "*A Review of High-Resolution X-ray Computed Tomography and Other Imaging Modalities for Small Animal Research*", Lab Animal, Vol. 30, No. 3, pp. 36-45, 2001.

[2] Cherry S.R., Shao Y., Silverman R.W., Meadors K., Siegel S., Chatziioannou A., Young J.W., Jones W., Moyers J.C., Newport D., Boutefnouchet A., Farquhar T.H., Andreaco M., Paulus M.J., Binkley D.M., Nutt R., and Phelps M.E., "*MicroPET: A High Resolution PET scanner for Imaging Small Animals*", IEEE Trans. Nucl. Sci., Vol. 44, No. 3, pp. 1161-1166, 1997.

[3] David P. McElroy, Lawrence R. MacDonald, Freek J. Beekman, Yuchuan Wang, Bradley E. Patt, Jan S. Iwanczyk, Benjamin M. W. Tsui, and Edward J. Hoffman, "*Performance Evaluation of A-SPECT: A High Resolution Desktop Pinhole SPECT System for Imaging Small Animals*", IEEE Trans. Nucl. Sci., Vol. 49, No. 5, pp. 2139-2147, 2002.

[4] Masaya Takahashi, David B. Hackney, Guixin Zhang, Suzanne L. Wehrli, Alex C. Wright, William T. O'Brien, Hidemasa Uematsu, Felix W. Wehrli, and Michael E. Selzer, "*Magnetic resonance microimaging of intraaxonal water diffusion in live excised lamprey spinal cord*", Proc. Natl. Acad. Sci., Vol. 99, No. 25, pp. 16192-16196, 2002.

[5] S. C. Lee, M. H. Cho, and S. Y. Lee, "*Performance Comparison of Reconstruction Algorithms for Fan-Beam Computerized Tomography*", J. Biomed. Eng. Res., Vol. 22, No. 3, pp. 223-229, 2001.

[6] G. N. Ramachandran, and A. V. Lakshminarayanan, "*Three dimensional reconstructions from radiographs and electron micrographs: application of convolution instead of Fourier transforms*", Proc. Natl. Acad. Sci., Vol. 68, pp. 2236-2240, 1971.

[7] Ed. S. Webb, The Physics of Medical Imaging, Inst. of Phys. Pub., pp. 123-131, 1988.

[8] Holdsworth D W, Drangova M, Fenster A, "*A high-resolution XRII-based quantitative volume CT scanner*", Med. Phys., Vol. 20, No. 2, pp. 449-462, 1993.

[9] Jiang Hsieh, Computed Tomography: Principles, Design, Artifacts, and Recent Advances, Bellingham: SPIE Press, pp. 265-276, 2003.

[10] C. H. McCollough, F. E. Zink, Performance evaluation of CT systems, Categorical Courses in Diagnostic Radiology Physics, pp. 189-207, 2000.